ACS APPLIED ENERGY MATERIALS

Article

Cite This: ACS Appl. Energy Mater. 2020, 3, 573−585

www.acsaem.org

Stable and Highly Conductive Polycation−Polybenzimidazole Membrane Blends for Intermediate Temperature Polymer Electrolyte Membrane Fuel Cells

Gokul Venugopalan,[†] Kevin Chang,[‡] Justin Nijoka,[†] Sarah Livingston,[†] Geoffrey M. Geise,[‡] and Christopher G. Arges*[,†]

[†]Cain Department of Chemical Engineering, Louisiana State University, Baton Rouge, Louisiana 70803, United States

[‡]Department of Chemical Engineering, University of Virginia, Charlottesville, Virginia 22904, United States

Supporting Information

ABSTRACT: Intermediate-temperature polymer electrolyte membrane fuel cells (IT-PEMFCs), operating with phosphoric acid (H_3PO_4) doped polybenzimidazole (PBI), are severely limited by H_3PO_4 evaporation at high temperatures and poor resiliency in the presence of water. Polycations (PCs), on the other hand, provide good acid retention due to strong ion-pair interactions but have low conductivity due to lower ion-exchange capacity when compared to PBI. In this work, a class of H_3PO_4 doped PC−PBI membrane blends was prepared, and the optimal blend (50:50 ratio) exhibited remarkably high in-plane proton conductivity, near 0.3 S cm^{-1} at 240 °C, while also displaying excellent thermal stability and resiliency to water vapor. Microwave dielectric spectroscopy demonstrated that incorporating PBI into the PCs raised the dielectric constant by 50−70% when compared to the PC by itself. This observation explains, in part, the high proton conductivity of the optimal membrane blend. Finally, an all-polymeric membrane electrode assembly with the new materials gave a competitive IT-PEMFC performance of 680 mW cm^{-2} at 220 °C under dry H_2/O_2. Importantly, the cell was stable for up to 30 h at 220 °C and over 84 h at 180 °C. The IT-PEMFC had reasonable performance (450 mW cm^{-2}) with 25% carbon monoxide in the hydrogen fuel.

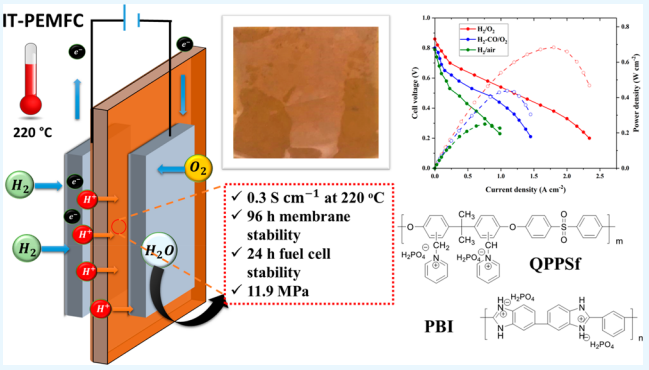

KEYWORDS: *fuel cells, polymer electrolyte membranes, intermediate temperature, microwave dielectric spectroscopy, hydrogen from steam-reformed methane*

1. INTRODUCTION

Low temperature polymer electrolyte membrane fuel cells (LT-PEMFCs; <100 °C) are part of a clean energy technology portfolio because they only emit water when reacting hydrogen (H_2) fuel with oxygen (O_2) from terrestrial air. Furthermore, they convert fuel with greater efficiency when compared to traditional heat engines. LT-PEMFCs have experienced steady improvement over time in terms of performance, efficiency, cost competitiveness, and stability.[1,2] The previous track record of LT-PEMFC improvement, catalyzed by collaborations from researchers in academia, national laboratories, and industry, suggests that this technology may eventually achieve ambitious metrics set by the U.S. Department of Energy Fuel Cell Technologies Office (e.g., 65% efficiency, <$30 kW_{net}^{-1} stack costs (when manufactured at >0.5 million units per year), and durability of greater than 8,000 h).[3] However, marketplace success for LT-PEMFCs could be stymied by the high costs associated with ultrapure H_2 fuel, which is currently ~$5 to 8 GGE^{-1} (gallon of gas equivalent) when produced from water electrolysis.[4] Powering fuel cells with H_2 derived steam-reformed methane (SRM) could offer significant cost savings (~$2 GGE^{-1}) that would translate to marketplace competitiveness for LT-PEMFCs.[4] Despite the advantages of H_2 from SRM, it contains pollutants, such as carbon monoxide (CO) and sulfur dioxide (SO_2), that poison electrocatalyst surfaces (<120 °C) jeopardizing LT-PEMFC performance.[5,6]

Over the past 30 years, intermediate temperature PEMFCs (IT-PEMFCs) based upon anhydrous proton conducting membranes have been prepared using phosphoric acid (H_3PO_4) doped polybenzimidazole (PBI).[1,7−14] These anhydrous proton conducting materials enable the fuel cell to operate above 120 °C. At the elevated temperatures, low cost H_2 fuel from SRM can be used because the electrocatalysts are more tolerant to CO and SO_2 pollutants.[8,15] An additional benefit of using an anhydrous proton conducting membrane is circumvention of an external humidifier that is used to hydrate

Received: September 12, 2019
Accepted: December 6, 2019
Published: December 6, 2019

DOI: 10.1021/acsaem.9b01802
ACS Appl. Energy Mater. 2020, 3, 573−585

the conventionally used perfluorosulfonic acid (PSFA) membranes and electrode binders in LT-PEMFCs. Hydration of PFSA is critical for promoting proton conductivity (κ_{H+}) and minimizing ohmic resistances within the cell.[16,17] Elimination of the external humidifier, and control systems to manage water within the cell, manifests a \$1 to \$7.5 kW_{net}^{-1} cost savings.[4,18] Furthermore, higher cell temperature enhances IT-PEMFC efficiency through better heat rejection from the cell caused by larger temperature gradients. The better heat rejection shrinks (or potentially eliminates) the sizable radiator currently used in LT-PEMFC stacks for automotive applications. It is also worth mentioning that higher temperatures promote better redox kinetics in the electrode layers.[19]

As lucrative as IT-PEMFCs appear to be, acid-doped PBI has severe stability limitations in the presence of water and at temperatures greater than 160 °C.[20] The H_3PO_4 in PBI starts to evaporate at 180 °C, and any condensed water in contact with the H_3PO_4-doped PBI membrane supplants H_3PO_4 causing an eventual catastrophic drop in membrane conductivity. Kim and co-workers, and others,[21−23] over the past three years have examined H_3PO_4-doped polycation (H_3PO_4−PC) membranes and binders (note: PCs are typically used as anion exchange membranes for alkaline fuel cells) as a superior alternative to H_3PO_4−PBI for IT-PEMFCs.[24,25] The H_3PO_4−PC materials foster strong electrostatic interactions between the tethered cation moieties and the phosphate type anions enabling greater acid retention across the temperature range of 50 to 220 °C. Additionally, the tethered cation−phosphate anion interactions are more immune to water substitution when the cell is exposed to humified water at temperatures less than 100 °C. Compared to H_3PO_4−PBI, the electrostatic interaction between quaternary ammonium groups and phosphate anions in H_3PO_4−PC is 8× stronger than the acid−base interactions between benzimidazole and H_3PO_4.[26] Hence, the H_3PO_4−PC molecular design mitigates acid leaching in the presence of water and evaporation of H_3PO_4 at temperatures greater than 160 °C. With H_3PO_4−PC, Kim and co-workers have shown peak power densities as high as 870 mW cm^{-2} with oxygen and no humidification.[24] However, these data for IT-PEMFC above 200 °C used a H_3PO_4−PC ionomer electrode binder with a ceramic proton conducting membrane (i.e., only a partial polymeric membrane electrode assembly was used). It is important to note that ceramic membranes are not conducive to roll-to-roll manufacturing and cannot achieve small thickness values and mechanical resiliency that are on par with polymeric materials. Finally, our initial experiments with H_3PO_4−PC with different PC chemistries demonstrated substantially smaller κ_{H+} values than a commercially available PBI due to lower acid availability and lesser interaction sites (see Figure S1).

To overcome the H_3PO_4 evaporation in PBI and augment the acid uptake of PCs, we have prepared a new class of anhydrous proton conducting membranes based upon PC−PBI polymer blends doped with H_3PO_4. This new class of anhydrous proton conducting polymer blends gave impressive κ_{H+} values of ∼0.3 S cm^{-1} at 240 °C and excellent mechanical properties (11.9 MPa at break) in addition to good thermal stability for 4 days at 220 °C. Using the optimal blend of 50:50 PC−PBI, a fuel cell demonstration was carried out at the challenging temperature of 220 °C with an all polymeric membrane electrode assembly (MEA). An encouraging peak power density of 680 mW cm^{-2} with dry H_2/O_2 was achieved. Plus, the IT-PEMFC showed reasonable performance with 25% CO in the H_2 fuel stream, was stable over 24 h, and recovered its performance when switching from H_2−CO fuel back to pure H_2 fuel. However, it was uncovered that the free-standing membrane blends break at 30 h at 220 °C but can survive in the fuel cell for over 80 h at 180 °C. To understand the high κ_{H+} of PC−PBI blend, microwave dielectric spectroscopy revealed that the addition of PBI to the PC substantially raised the dielectric constant (ε') of the polymer materials. The increase in ε' was attributed to the large H_3PO_4 uptake. This effect, coupled with increased hydrogen bond frustration spurred by the PC, accounted for the remarkably high κ_{H+} values. The thermal stability of the PC−PBI blend was ascribed to the electrostatic interactions that anchored the phosphate anions in the membrane in addition to the chemical stability of the aromatic backbones and cations in the polymer hosts.

2. EXPERIMENTAL SECTION

2.1. Chemicals. Polysulfone (PSf) M.W. 60,000 − Acros organics, chloroform ($CHCl_3$) − ACS grade − VWR, chlorotrimethylsilane − VWR, paraformaldehyde − reagent grade − Sigma-Aldrich, tin(IV) chloride ($SnCl_4$) − Sigma-Aldrich, methanol (MeOH) − ACS grade − Fisher Scientific, polybenzimidazole (PBI) 10% in DMAc − PBI solutions Inc., N,N-dimethylacetamide − ACS grade − Alfa Aesar, chloroform D 99.8% ($CDCl_3$) − Alfa-Aesar, pyridine − ACS grade − VWR, 85 wt % phosphoric acid (H_3PO_4) − ACS grade − VWR, standardized 1 M NaCl − VWR, standardized 1 M NaOH − VWR, phenolphthalein indicator 1% in ethanol − VWR, reagent alcohol (90% ethanol, 5% methanol, and 5% 2-propanol), Pt/C (37.3% on higher surface area carbon) − Tanaka Kikinzoku International.

2.2. Synthesis of CMPSf. CMPSf was prepared by Friedel−Crafts reaction as reported by Arges et al.,[27] but with a slight modification to the procedure. Ten grams of Udel poly(arylene ether) sulfone (PSf) was dissolved in 500 mL of chloroform ($CHCl_3$). The reaction was carried out in a round-bottom flask equipped with a magnetic stirred and a reflux condenser. After the PSf dissolved, 6.8 g of paraformaldehyde was added followed by 30 mL of chlorotrimethylsilane. The bulb flask was blanketed with nitrogen and sealed with a rubber septum. 525 μL of $SnCl_4$, the Lewis acid catalyst, was added slowly to the bulb flask using a syringe punctured through the septum.

The extent of chloromethylation was monitored during the reaction until the desired degree of functionalization (DF) value of chloromethyl groups per repeat unit was achieved. The DF value was monitored by ^{1}H NMR during the reaction. The reaction solutions, either collected at the end of the reaction or withdrawn during the reaction, were cooled to room temperature and poured into methanol (5:1 volume ratio of methanol to reaction solution) to precipitate the polymer out of solution. The precipitated polymer was collected by vacuum filtration and vacuum-dried. The CMPSf was purified further by dissolving it in $CHCl_3$ (5 wt %) followed by precipitating in methanol and vacuum filtering and drying the solid using the aforementioned procedure. Figure S2 reports the ^{1}H NMR of CMPSf.

2.3. Preparation of Blended and Nonblended Membranes. CMPSf was dissolved in DMAc to attain a 5 wt % solution. Similarly, a 5 wt % solution of PBI in DMAc was prepared. PBI was added to CMPSf at different volume ratios to achieve a desired CMPSf−PBI blend composition. The ratios examined were 0, 30, 40, 50, 60, and 100%. 0% refers to PBI only, and 100% refers to CMPSf only. The solutions were sonicated for 10 min and drop cast on a glass plate on a leveled surface in an oven at 120 °C for 6 h. After peeling of the membranes from the glass plate, the blended membranes that featured CMPSf were then immersed in pyridine solution (1 M in reagent alcohol) at 40 °C for 16 h to convert the chloromethylated groups in PSf to quaternary benzylpyridinium chloride groups. Then, the resultant membranes were washed excessively with DI water to remove unreacted pyridine and were blot dried. The thickness of the dry membranes ranged from 32−68 μm. Figure S3 provides the ^{1}H NMR spectrum that confirms the chloromethyl group conversion to

DOI: 10.1021/acsaem.9b01802
ACS Appl. Energy Mater. 2020, 3, 573−585

quaternary benzylpyridinium chloride for QPPSf only (i.e., no PBI added). The acid doping of PBI and QPPSf–PBI blended membranes was done by immersing membranes in 85 wt % phosphoric acid (H_3PO_4) at 120 °C for 6 h.[26] QPPSf was doped with 85 wt % phosphoric acid (H_3PO_4) at 25 °C because immersion of this membrane in this acid at 120 °C for 1 h dissolved the membrane (note: Y. S. Kim and co-workers doped their PC membranes with H_3PO_4 at room temperature).[26] After acid doping, the membranes were then blot dried for removing the excess acid from the surface.

2.4. H_3PO_4 Uptake and Amount per Base Moiety and Calculation of QPPSf IEC. The H_3PO_4 uptake values of QPPSf, PBI, and their blends were observed by measuring their weight change before and after immersing in 85 wt % H_3PO_4.[26] The total H_3PO_4 uptake by the membrane was calculated using eq 1:

$$H_3PO_4 \text{ uptake} = \frac{W_2 - W_1}{W_1} \tag{1}$$

where W_1 and W_2 are the weight of the polymer membrane before and after doping.

The IEC of the pristine QPPSf membrane (i.e., not H_3PO_4 doped and not blended) was determined using ^{1}H NMR spectroscopy.[27] First, the degree of functionalization (DF) of CMPSf was calculated using ^{1}H NMR:

$$DF = \frac{2 \times \text{Area}_{CH_2Cl \text{ substituent}}(4.5 \text{ ppm})}{\text{Area}_{PSf \text{ substituent}}(7.8 \text{ ppm})} \tag{2}$$

Conversion of chloromethylated sites to cation sites:

$$\text{Conversion} = \frac{\text{Area}_{\text{cation substituent}}(9.2 \text{ ppm})}{\text{Ratio} \times DF \times \text{Area}_{PSf \text{ substituent}}(1.8 \text{ ppm})} \tag{3}$$

$$\text{Ratio} = \frac{\#\text{of protons for cation substituent}}{\#\text{of protons for PSf substituent}} \tag{4}$$

Determining theoretical IEC of polycations

$$IEC\left(\frac{\text{mmol}}{\text{g}}\right) = \frac{DF \times 1000}{(MW_{PSf,\text{monomer}} + DF \times MW_{\text{cation}})}. \text{ Conversion} \tag{5}$$

$$MW_{\text{cation}} = (MW_{\text{cation free base conjugate}} + MW_{\text{counteranion}} + MW_{CH2} - 1)$$

The IEC values of the non-H_3PO_4 doped membrane blends (QPPSf–PBI) were determined by performing a weighted average between the known IEC of QPPSf and the known IEC of PBI. The IEC of the non-H_3PO_4-doped membranes represents the IEC (base moiety basis).

The H_3PO_4 level per repeat unit (X) was determined using eq 6 and by titrating the released H_3PO_4 from acid-doped membranes. For this procedure, the H_3PO_4-doped membranes were immersed in standardized 1 M NaCl for 48 h to exchange acid in the membrane with sodium ions. The membranes were taken out after 48 h. The acid in solution was titrated against standardized 1 M NaOH (N_{NaOH}) to the end point with phenolphthalein as the indicator. The volume used for the titration to the end point, V_{NaOH}, was recorded. W_{dry} was the weight value of the H_3PO_4-doped membrane.

The number of H_3PO_4 per repeat unit of PBI, QPPSf, and blended membranes was determined by eq 6:

$$H_3PO_4 \text{ level per repeat unit (X)} = \frac{V_{NaOH} \times N_{NaOH}}{(\text{Equiv}_{mol} \times ({}^{w_{dry}}/_{M_w}))} \tag{6}$$

Equiv_{mol} of H_3PO_4 for NaOH (which is 3), M_w is the weighted average of the individual polymer repeat unit's molecular weight.

Number of H_3PO_4 per base moiety (nH_3PO_4 B^{-1}) was found by

$$nH_3PO_4\ B^{-1} = \frac{X \times 1000}{IEC_B \times M_w} \tag{7}$$

M_w is the weighted average of the individual polymer repeat units' molecular weight values.

2.5. κ_{H+} Measurements. In-plane κ_{H+} measurements were carried out in a 4-point platinum probe with PTFE housing (Bekktech conductivity cell) and using galvanostatic electrochemical impedance spectroscopy (EIS) using a Gamry 3000 AE8 channel potentiostat over frequency range of 1 MHz to 1 Hz with a current perturbation of 0.1 mA. The κ_{H+} measurements were carried out in a temperature-controlled gravity oven in the temperature range of 100–250 °C. The cross-sectional area of the membrane samples was 1 × 3 cm^2. The κ_{H+} of the membrane samples was calculated using eq 8:

$$\kappa_{H+} = \frac{L}{R \times D \times W} \tag{8}$$

where L (cm) is the distance between the electrodes, R (Ω) is the resistance of the membrane, D (cm) is the thickness of the membrane, and W (cm) is the width of the membrane.

Through-plane κ_{H+} measurements were carried out in the 850 E Scribner Associates, Inc. Fuel Cell Test Station. The EIS was performed in the fuel cell over the frequency range of 1 kHz to 0.1 Hz with a current perturbation of 0.1 mA. The κ_{H+} of the membrane samples was calculated using eq 9:

$$\kappa_{H+} = \frac{D}{\text{HFR} \times A} \tag{9}$$

where D (cm) is the thickness of the membrane, A (cm^2) is the area of the membrane electrode assembly (MEA), and HFR (Ω-cm^2) is the high frequency resistance obtained from EIS plot.

2.6. Scanning Electron Microscopy. The microstructure of the 50:50 QPPSf–PBI membrane was studied using scanning electron microscopy (SEM). The instrument settings were a back scattered electron detector, working distance of 5.7 mm, and an accelerating voltage of 10 keV. EDX spectra were collected in different regions (PBI and QPPSf) of the electron micrograph image. Sample preparation for SEM entailed infiltrating the membrane with chloroplatinate anions ($PtCl_6^-$) by immersing the membrane sample in potassium chloroplatinate (1 M K_2PtCl_6 in DI water) for 3 h followed by rinsing with excessive water to remove K_2PtCl_6 from PBI. Because this salt solution contains no acid, the PBI is not protonated and does not pair with $PtCl_6^-$.

2.7. Microwave Dielectric Spectroscopy. The relative permittivity properties of PBI, QPPSf, and their blends with and without H_3PO_4 were characterized from 0.045 to 26.5 GHz using a calibrated Keysight N9928A Vector Network Analyzer (VNA).[28] Membrane samples were cut into rectangular-shaped strips that were approximately 0.5 cm wide. These strips were wrapped around the center conductor of a 3.5 mm diameter and 5 cm long coaxial transmission line, which acted as the sample holder, until enough sample was wrapped to fill the annular space between the conductor and the wall of the transmission line. The VNA transmits electromagnetic radiation through the sample holder and measures the intensity of the signal that is either transmitted or reflected by the sample. These measurements were recorded as frequency-dependent S-parameters. These S-parameters are related to the relative complex permittivity, ε^*, of the sample.[29,30] The real part of ε^* is the frequency-dependent relative permittivity, ε', which at low frequency, is often interpreted as the dielectric constant of the material.[30,31]

2.8. Assessment of Thermal Stability. The thermal stabilities of the membranes PBI, QPPSf, and QPPSf–PBI 50:50 were assessed via five different methods. The first method examined thermal stability cycling by placing the membrane sample in the Bekktech conductivity cell in the gravity oven followed by ramping up the temperature from 100–250 °C. Individual temperature points were held while performing an EIS measurement. After carrying out the EIS at 250 °C, the oven was cooled to 100 °C and then reheated to 250 °C using the same ramp up and temperature hold (during EIS measurement) protocol. The results from the EIS were used to compute the κ_{H+}. The goal was to perform three cycles to assess conductivity losses for PBI, QPPSf, and 50:50 QPPSf–PBI membrane. However, the PBI and QPPSf did not survive the first heating cycle.

DOI: 10.1021/acsaem.9b01802
ACS Appl. Energy Mater. 2020, 3, 573–585

Scheme 1. Method to Prepare QPPSf–PBI Membrane and Ionomer Electrode Binder Blends That Provide Anhydrous, High Temperature Proton Conduction

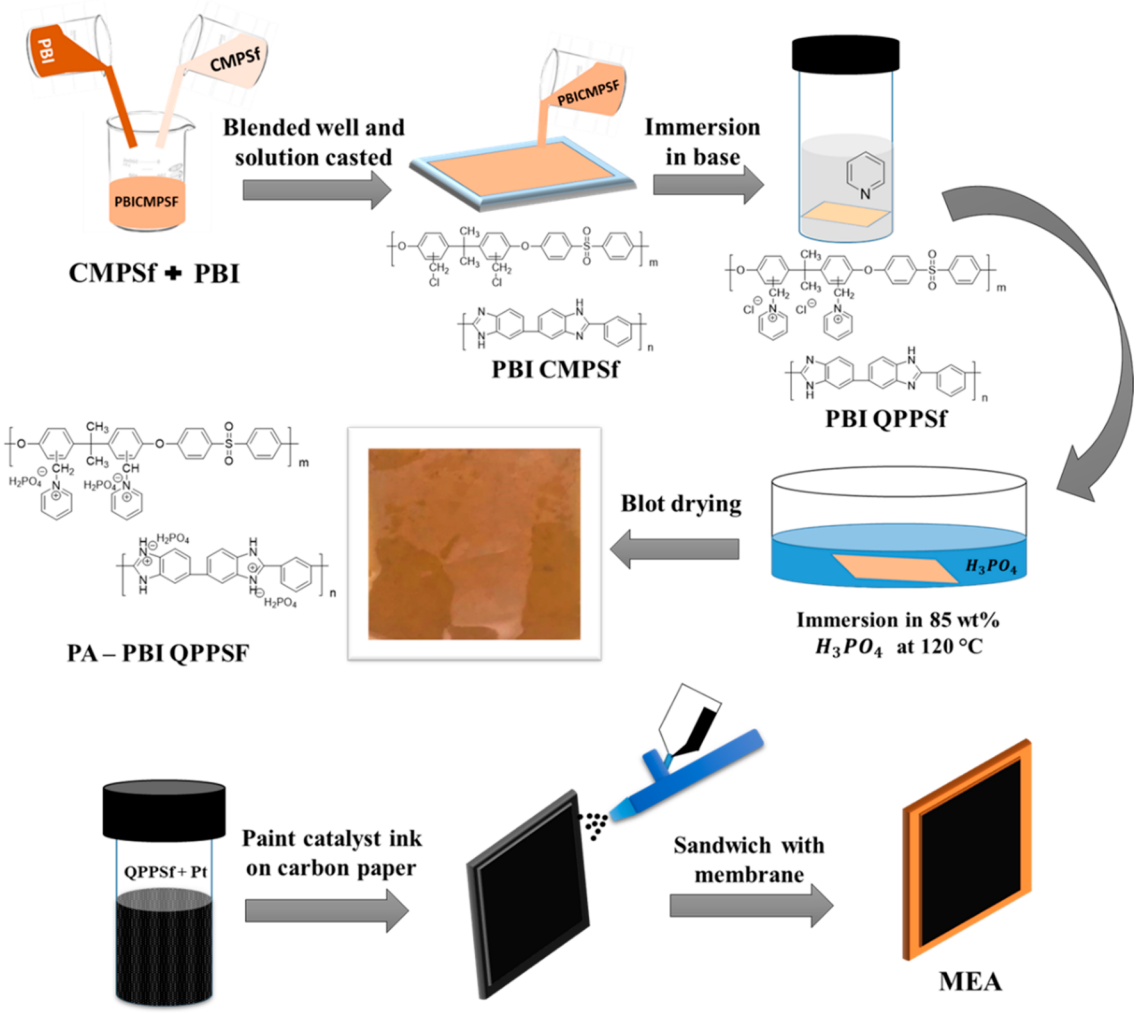

The second thermal stability assessment monitored changes in κ_{H+} of 50:50 QPPSf–PBI at 220 °C for 96 h. This sample was only evaluated because PBI and QPPSf were shown to be unstable once the temperature of 200 °C was attained.

The third stability assessment examined the changes in membrane weight for all the membrane samples when holding the samples at 220 °C for 48 h in a gravity oven. The change in membrane weight before and after the temperature hold was gravimetrically determined.

The fourth stability test investigated the membranes' tolerance to humidity at 80 °C/40% RH. The changes in the membrane weight before the test and after the test were determined gravimetrically. For the test, the membrane sample was first placed in a Bekktech 4-point conductivity cell, which was then loaded into a Fuel Cell Technologies hardware setup plumbed to 850 E Scribner Fuel Cell Test Stand to control the temperature and humidity of the membrane sample.

The fifth and final thermal stability assessment performed TGA of 50:50 QPPSf–PBI with and without doping with H_3PO_4 under nitrogen using Pyris 1 TGA (TA Instruments). The samples were initially heated to 100 °C and equilibrated at that temperature for 10 min. Then, the samples' temperature was heated up to 700 °C at the rate of 10 °C min $^{-1}$. The change in weight of the sample was monitored during the heating from 100 to 700 °C.

To understand the stability of quaternary pyridinium groups in 50:50 QPPSf–PBI, TGA of pristine QPPSf and 50:50 QPPSf–PBI was performed. Also, QPPSf and 50:50 QPPSf–PBI were thermally treated at 220 °C for 48 h. These thermally treated membranes were then immersed in 85 wt % H_3PO_4 for acid uptake. The acid retention values of thermally treated QPPSf and 50:50 QPPSf–PBI were calculated. Furthermore, the κ_{H+} of thermally treated and untreated (pristine) membranes doped with 85 wt % H_3PO_4 were calculated at 25 °C, 50 °C, and 100 °C.

2.9. Mechanical Properties. The stress–strain curves of the membranes doped with H_3PO_4 were measured using a INSTRON 3365 (25 °C) and TA Instruments Dynamic Mechanical Analyzer operated in Tensile Test Mode (220 °C). The strain rate during the test was 2 mm min^{-1}. The measurements were carried out at 25 and 220 °C in an ambient environment (~50% relative humidity). Prior to the measurements, the membrane samples were equilibrated at 120 °C overnight to remove the water from the system. The time between doping the acid with membranes and performing the tensile test was short enough to negate the humidity effect on the membranes.

2.10. Preparation of GDEs. Catalyst inks were first prepared by mixing 0.2 g of carbon supported catalyst (37% Pt on high surface area carbon, Tanaka Kikinzoku International) with 1.715 g of QPPSf ionomer solution dissolved in approximately 5.5 g of reagent alcohol. This catalyst ink gave the best fuel cell performance. The prepared ink was stirred for 10 min and sonicated for 30 min. The GDE was prepared by painting the ink on a carbon-based gas diffusion layer (GDL) with an aerosolized spray gun (nitrogen gas). The active area of the resultant GDE was 5 cm^2. The catalyst loading was determined gravimetrically by weighing the GDL prior to spray deposition and after depositing the catalyst layer and drying the electrode. The catalyst loading was maintained as 0.5 mg_{Pt} cm^{-2} for each GDE (one

DOI: 10.1021/acsaem.9b01802
ACS Appl. Energy Mater. 2020, 3, 573–585

used as the anode and the other as the cathode). The weight fraction of the ionomer in the electrode layer was 30 wt %. The GDEs were then immersed in 85 wt % H_3PO_4 for 10 min. The short immersion time was done to prevent excess H_3PO_4 uptake in the electrodes that causes poor mass transfer in the GDE layers. An alternative catalyst ink was prepared in identical fashion except that CMPSf and PBI were used in a 50:50 weight ratio of 1.715 g total and the solvent was DMAc. After painting the catalyst ink onto the GDLs with this formulation, the resultant GDEs were immersed in pyridine solution (1 M in reagent alcohol) to convert the chloromethylated groups in PSf to quaternary benzylpyridinium chloride groups. Then the electrodes were immersed in H_3PO_4 for acid uptake using the same procedure.

2.11. MEA Fabrication and Fuel Cell Testing. For the fuel cell tests, a MEA was prepared by placing the acid-doped QPPSf−PBI 50:50 blended membrane between two identical GDE's that were housed with rubber gaskets. The MEA was then sandwiched between graphite serpentine flow fields and gold current collectors in a Fuel Cell Technologies Hardware setup (5 cm^2 geometric area). The assembled single-cell was plumbed to a 850 E Scribner Associates, Inc. Fuel Cell Test Station. Then, a homemade fiberglass housing was placed over the fuel cell hardware for insulation followed by heating the cell to 220 °C (note: the insulation is required to stabilize the cell temperature). Then, dry nitrogen was passed on the anode and cathode side (note: the humidifier was bypassed for both gas feeds). Then, nonhumidified H_2/O_2, H_2-CO/O_2, or H_2/air was passed into the fuel cell at a minimum flow rate of 0.2 l SLPM at a stoichiometric ratio of 1.2× and 2× for the anode and cathode, respectively. 161 kPa of back pressure (absolute pressure) was applied to both the anode and cathode. The polarization curves were collected every 0.05 V by holding the voltage for 1 min. The EIS was performed in the fuel cell test stand over frequency range of 1 kHz to 0.1 Hz with a current perturbation of 0.1 mA.

Stability tests were performed by continuous supply of dry H_2/O_2 for 2 h, followed by H_2-CO/O_2 for 6 h, and then 18 h of dry H_2/O_2. The cell voltage was held to 0.4 V (T = 220 °C) during the 24 h stability assessment. The polarization curves with dry H_2/O_2 were recorded before and after the stability tests. Furthermore, a longer stability assessment was performed for the IT-PEMFC under a different protocol as reported by Li et al.[32] In this protocol, the cell was operated at a constant current at 0.2 A cm^{-2} and no back pressure was applied, and the IT-PEMFC stability was evaluated at different temperatures over 116 h.

3. RESULTS AND DISCUSSION

3.1. Preparation of H_3PO_4-Doped 50:50 QPPSf−PBI Membranes. Scheme 1 depicts the method to prepare the PC−PBI blends that resulted in mechanically robust, free-standing membranes. The scheme also illustrates a pathway to yield stable solutions of chloromethylated Udel polysulfone (CMPSf)−PBI, of varying ratios, that can be further processed into ionomer electrode binders. The chloromethyl groups in CMPSf are converted into quaternary benzylpyridinium cations (QPPSf) with a chloride counterion by immersing the membrane or gas diffusion electrodes (GDEs) into 1 M pyridine in reagent alcohol. Quaternary benzylpyridinium was selected over quaternary benzyl trimethylammonium (or other alkyl ammoniums) because its aromatic structure provides greater oxidative stability.[33] The polyaromatic backbone and aromatic cation were employed to withstand the high temperature environment of the cell. During fuel cell operation, reactive oxygen species are generated at the cathode, and these species spur polymer degradation (with the worst-case scenario[34] being at elevated temperatures, dry conditions, and OCV).

To determine if CMPSf and PBI could cross-link while drop casting and drying the mixed polymer solution, the prepared 50:50 CMPSf−PBI membrane blend was immersed in DMAc, DMSO, and NMP. The 50:50 CMPSf−PBI blend dissolved in each one of the solvents (5 wt %; see Figure S4). Furthermore, the H_3PO_4 doped 50:50 CMPSf−PBI membrane κ_{H+} and thermal stability were compared against QPPSf−PBI (see Figure S5). The 50:50 QPPSf−PBI displayed better acid retention and higher κ_{H+} compared to 50:50 CMPSf−PBI because it contained pyridinium moieties that promoted acid retention. The retention of acid improved κ_{H+} − in particular at higher temperatures. If the 50:50 CMPSf−PBI was cross-linked, which could occur by the chloromethyl groups reacting with benzimidazole,[35] it would contain tethered benzimidazolium cation moieties that would retain acid and promote κ_{H+} like 50:50 QPPSf−PBI. The fact that CMPSf−PBI was soluble in the aforementioned solvents and that it has poor acid retention and κ_{H+} when doped with H_3PO_4 signified that CMPSf and PBI were not cross-linked.

Different blends of PC−PBI membranes were prepared to identify the composition that would yield the best κ_{H+}, while also satisfying stability constraints at temperatures above 200 °C and in the presence of water. The data presented in subsequent sections focuses on 50:50 QPPSf−PBI blend ratio in relation to PBI and QPPSf alone because this ratio resulted in the best membrane properties. The other blended membrane ratios are presented in the Supporting Information. Furthermore, all polymer notation for the remainder of this report infers that the materials have been doped with H_3PO_4 (unless otherwise noted). It is important to note that blending 5 wt % QPPSf in DMAc with 5 wt % PBI in DMAc, at any ratio during the preparation of the membranes, immediately resulted in gelation.

3.2. H_3PO_4 Uptake and per Base Moiety and IEC Values. Table 1 reports the H_3PO_4 uptake, H_3PO_4 per base moiety (nH_3PO_4 B^{-1}) in the membrane, and the ion-exchange capacity (IEC) values for PBI, QPPSf, and 50:50 QPPSf−PBI on a base moiety basis (IEC). Table S1 provides these values for the QPPSf−PBI blends at other ratios. The IEC of QPPSf in the chloride counterion form is 1.7 mequiv g^{-1}, and for PBI (i.e., benzimidazole) it is 6.5 mequiv g^{-1}.[10,26] IEC values for the blended membranes were found using weighted averages of the individual IEC values of PBI and QPPSf. The IEC of 50:50 QPPSf−PBI blend was 4.1 mequiv g^{-1}. The H_3PO_4 uptake of QPPSf was 180%, whereas for PBI it was 295%. The higher acid uptake of PBI was due to its higher IEC when compared to QPPSf. The 50:50 QPPSf−PBI blend had a H_3PO_4 uptake of 220% and this corresponded to a 7.9 H_3PO_4 B^{-1}. This value was smaller than PBI (9.4 H_3PO_4 B^{-1}) and QPPSf (9.3 H_3PO_4 B^{-1}). The 50:50 QPPSf−PBI blend had a smaller nH_3PO_4 B^{-1} value because its IEC was 2.4× higher than pristine QPPSf, but

Table 1. Physical and Mechanical Properties of H_3PO_4-Doped PBI, QPPSf, and 50:50 QPPSf−PBI

Sample	H_3PO_4 uptake (%)	IEC (mequiv g^{-1})	nH_3PO_4 B^{-1}	Ultimate tensile strength (MPa)[a]	Elongation at break (%)[a]
PBI	295	6.5	9.4	8.2	33
QPPSf	180	1.7	9.3	2.0	28
50:50 QPPSf−PBI	220	4.1	7.9	11.9	25

[a]Measurements conducted at ambient conditions: 25 °C and ∼50% relative humidity.

DOI: 10.1021/acsaem.9b01802
ACS Appl. Energy Mater. 2020, 3, 573−585

its H_3PO_4 uptake in relation to QPPS was only 1.2× greater. The high value of the nH_3PO_4 B^{-1} for PBI was due to its large acid uptake.

3.3. Mechanical Properties. Table 1 also reports the tensile strength and elongation at break of the 50:50 QPPSf–PBI, QPPSf, and PBI. Figure S6a and Table S1 show and report the results from tensile test measurements of the other QPPSf–PBI polymer blends at 25 °C. 50:50 QPPSf–PBI had the highest mechanical strength among all the other blends. However, the tensile test measurement of the 50:50 QPPSf–PBI membrane at 220 °C (see Figure S6b) showed a substantial loss in mechanical strength of the membrane (from 11.9 MPa at 25 °C to 2 MPa at 220 °C). The excellent mechanical strength of the 50:50 QPPSf–PBI blend at 25 °C may be due to the phase separation of the different polymers at the micron-size level that was observed via electron microscopy (see Figure S7). The phase separation was substantiated by the electron micrograph, and this phase separation explains why the blended membranes have a slightly cloudy appearance to them.

The tensile properties of the membranes will depend on the amount of phosphoric acid present in the membranes in addition to other factors such as temperature and humidity. The variation of ultimate tensile strength with acid uptake (%) of the membranes is shown in Figure S8. The mechanical strength of the 50:50 QPPSf–PBI was the highest, and this was attributed to the lower acid uptake of this membrane variant. Improving the toughness of the membrane is important for IT-PEMFCs because the membrane can better tolerate back pressure applied to the anode and/or the cathode without concern of puncturing the membrane that would lead to catastrophic cell behavior (e.g., mixed overpotentials).

3.4. κ_{H+} Conductivity and Microwave Dielectric Spectroscopy. Proton conductivity, κ_{H+}, is a critical membrane property for the IT-PEMFCs because the ohmic overpotential, for any fuel cell device, is linearly proportional to the area-specific resistance, which is inversely proportional to the proton conductivity (i.e., ASR = membrane thickness/κ_{H+}). At high current densities, a high ASR can severely compromise IT-PEMFC efficiency.

Figure 1a shows the anhydrous κ_{H+} of PBI, QPPSf, and 50:50 QPPSf–PBI from 25 to 240 °C. Figure S9 shows the anhydrous κ_{H+} of the other QPPSf–PBI blends. A very high κ_{H+} value, near 0.3 S cm^{-1}, was attained with the 50:50 QPPSf–PBI at 240 °C. Conversely, a commercially available PBI membrane displayed about half the κ_{H+} (0.1 S cm^{-1}) at 180 °C in comparison to the 50:50 QPPSf–PBI blend. Additionally, the PBI membrane experienced a drop in κ_{H+} at temperatures above 180 °C and eventual complete loss κ_{H+} when maintained at temperatures above 180 °C for a few minutes. Similarly, QPPSf membrane gave a maximum κ_{H+} of 0.09 S cm^{-1} at 200 °C (less than half of the 50:50 QPPSf–PBI blend); and like PBI, QPPSf's κ_{H+} severely deteriorated when increasing the temperature to 200 °C. It is important to point out that QPPSf swelled quite a bit during the H_3PO_4 imbibing step, which occurred at 25 °C. Immersion of the QPPSf in 85 wt % H_3PO_4 at 120 °C for one hour resulted in membrane dissolution. Plus, the QPPSf had a significant mass uptake of 180% after immersing in 85 wt % H_3PO_4 at 25 °C. Although a lower IEC of QPPSf may curtail swelling when doping it with H_3PO_4, it will have the undesired consequence of lower κ_{H+} values because of the smaller concentration of fixed ionic groups along the polymer backbone. To ensure that the κ_{H+} values were not inflated due to residual H_3PO_4 being present at the membrane surface, the in-plane and through-plane κ_{H+} values of the 50:50 QPPSf–PBI were compared (see Figure S10). The through-plane κ_{H+} is about 20% lower compared to in-plane κ_{H+} due to contact resistances at the electrode–electrolyte interface[36] and the fact that the membrane may have some anisotropy when it comes to proton conduction.

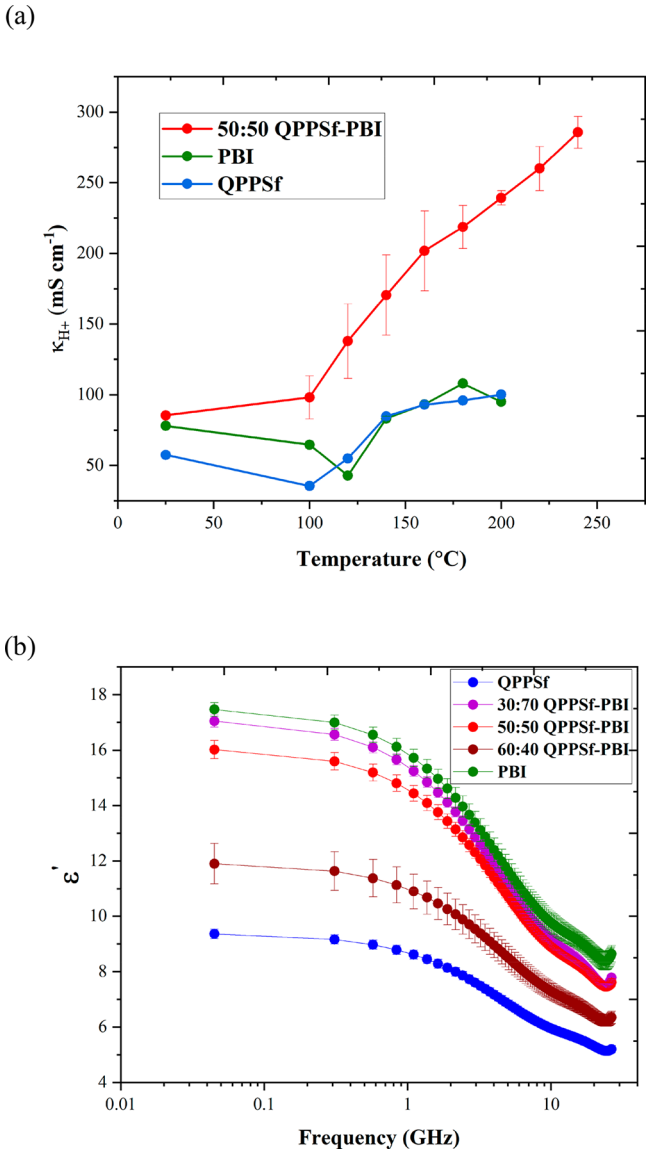

Figure 1. (a) In-plane proton conductivity (κ_{H+}) for PBI, QPPSf, and 50:50 QPPSf–PBI. (Note: the error bars are very small in the traces.) (b) Dielectric constant (ε') for these samples as a function of frequency.

Figure S11 shows the activation enthalpy calculation plot for QPPSf, PBI, and 50:50 QPPSf–PBI membranes. The activation enthalpy and pre-exponential values are reported in Table S2. It was observed that 50:50 QPPSf–PBI had the highest activation enthalpy compared to PBI and QPPSf. This might be due to the increased network frustration of protons in the blended membrane and the condensation of phosphoric acid to pyrophosphoric acid at higher temperatures.[37,38]

To better understand the proton conductivity properties of the different membranes, the dielectric constant (ε') of the membranes was measured using microwave dielectric spec-

DOI: 10.1021/acsaem.9b01802
ACS Appl. Energy Mater. 2020, 3, 573–585

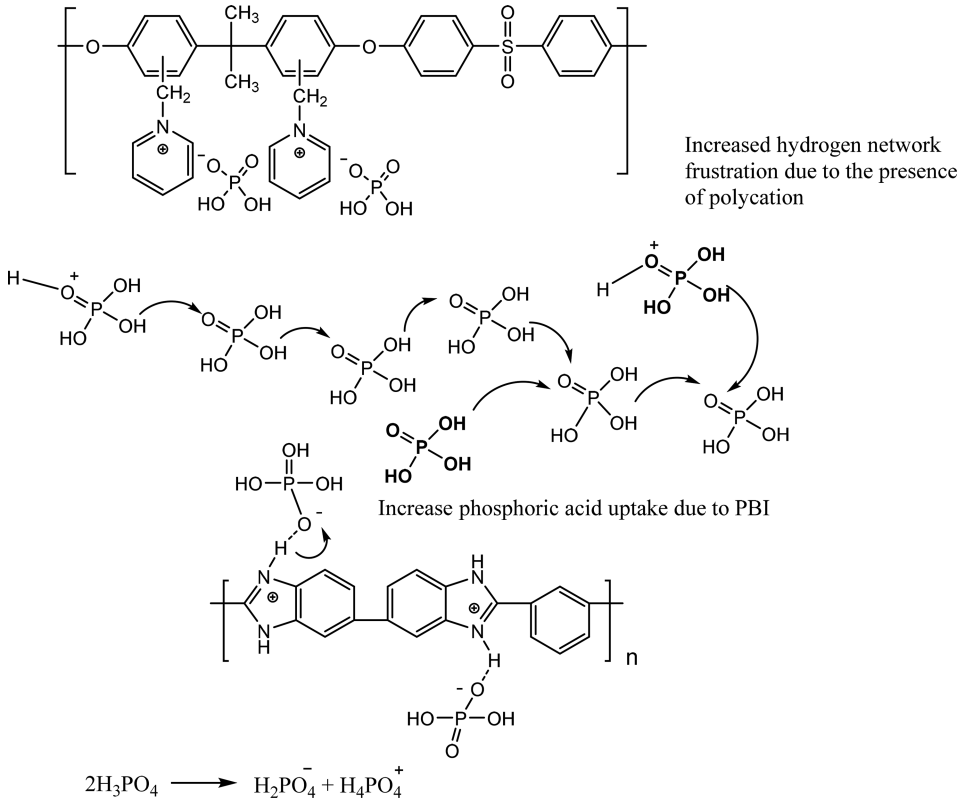

Figure 2. Schematic representation of phosphoric acid diffusion in 50:50 QPPSf–PBI.

troscopy. Chang et al. used microwave dielectric spectroscopy to examine the interplay of water content, ε', and ion sorption in hydrated polymers.[39] They reported that a fully hydrated PFSA (Nafion) had a ε' near 20, and this value was approximately a quarter of the value for water. Figure 1b reports the ε' response of the membranes as a function of frequency. Our analysis focused on the low frequency regime of Figure 1b as the ion dipoles in this frequency range are in phase with the microwave signal.[30] The dielectric constant, ε', for PBI was nearly a factor of 2 greater than that of QPPSf. Blending PBI into QPPSf at 50 to 70% caused an increase in the ε' values, and the ε' values of those materials were close to that of PBI. The measured ε' was taken to be proportional to the concentration of mobile ion dipoles in the polymer host, which is a proxy for the quantity of mobile H_3PO_4 groups present. Figure S12 shows that the ε' values increase when the membranes contain more H_3PO_4. Larger populations of mobile H_3PO_4 in the membrane help enable higher κ_{H+} values.

Hydrogen bonding, structural proton diffusion, and condensation of H_3PO_4 to pyrophosphoric acid strongly influence κ_{H+} in H_3PO_4 electrolytes at high temperatures.[37,38] Plus, residual water present in the H_3PO_4-doped membranes can compromise κ_{H+}.[40] It is important to note that PBI is a strong Brønsted base and H_3PO_4 protonates the nitrogen in benzimidazole leading to a reduction in hydrogen bond frustration and a lower κ_{H+} in comparison to neat phosphoric acid.[8,38] In a PC host, the tethered cation cannot accept a proton; thus, hydrogen bond frustration is higher for PC doped with H_3PO_4 than PBI doped with H_3PO_4. It would seem that H_3PO_4 -doped PCs are better suited for promoting κ_{H+} because they foster more hydrogen bonding frustration, but it is important to consider that most anion exchange membranes, which are used for these materials IT-PEMs when doped with H_3PO_4, have lower IEC values when compared to PBI. Therefore, they tend to have smaller acid uptake values. The reduction in acid uptake prevents attainment of large κ_{H+} values despite greater hydrogen bonding frustration by the polycation. It is important to note that ionic conductivity scales linearly with the concentration of ionic charge carriers in the electrolyte. By blending PC with PBI, a compromise was struck as the PC promotes greater hydrogen bond frustration, while the PBI yields greater H_3PO_4 uptake.

Figure 2 shows the mechanism of κ_{H+} in QPPSf–PBI membrane blends. The figure drawn was inspired by Dippel et al.[41] Because of iso-neutrality constraints, $H_2PO_4^-$ pairs with the pyridinium cation in QPPSf leaving behind a free proton that can shuttle along the excess H_3PO_4 network through the Grotthuss mechanism. However, the Brønsted base in PBI interacts with the proton in H_3PO_4 leaving no free protons behind. This not only reduces the structural diffusion of protons but also reduces the condensation of phosphoric acid. This is one reason why PBI doped H_3PO_4 cannot achieve the same κ_{H+} as neat H_3PO_4.[38] Furthermore, higher temperatures above 200 °C lead to condensation of H_3PO_4 to pyrophosphoric acid.[40] In the case of the QPPSf–PBI blend, increased hydrogen network frustration and the formation of pyrophosphoric acid at elevated temperatures are believed to be the reasons why high κ_{H+} values are attained at temperatures above 180 °C. It is possible that the rate of H_3PO_4 condensation to pyrophosphoric acid may occur faster than evaporation of excess H_3PO_4 in the polymer host. Hence, the higher order acid electrolyte is retained in the polymer blend matrix for promoting κ_{H+} and why the blended material can have stability at temperatures of 200 to 220 °C.

3.5. Thermal Stability, Water Resiliency, and Acid Retention. A well-known challenge in IT-PEMFCs relates to

DOI: 10.1021/acsaem.9b01802
ACS Appl. Energy Mater. 2020, 3, 573–585

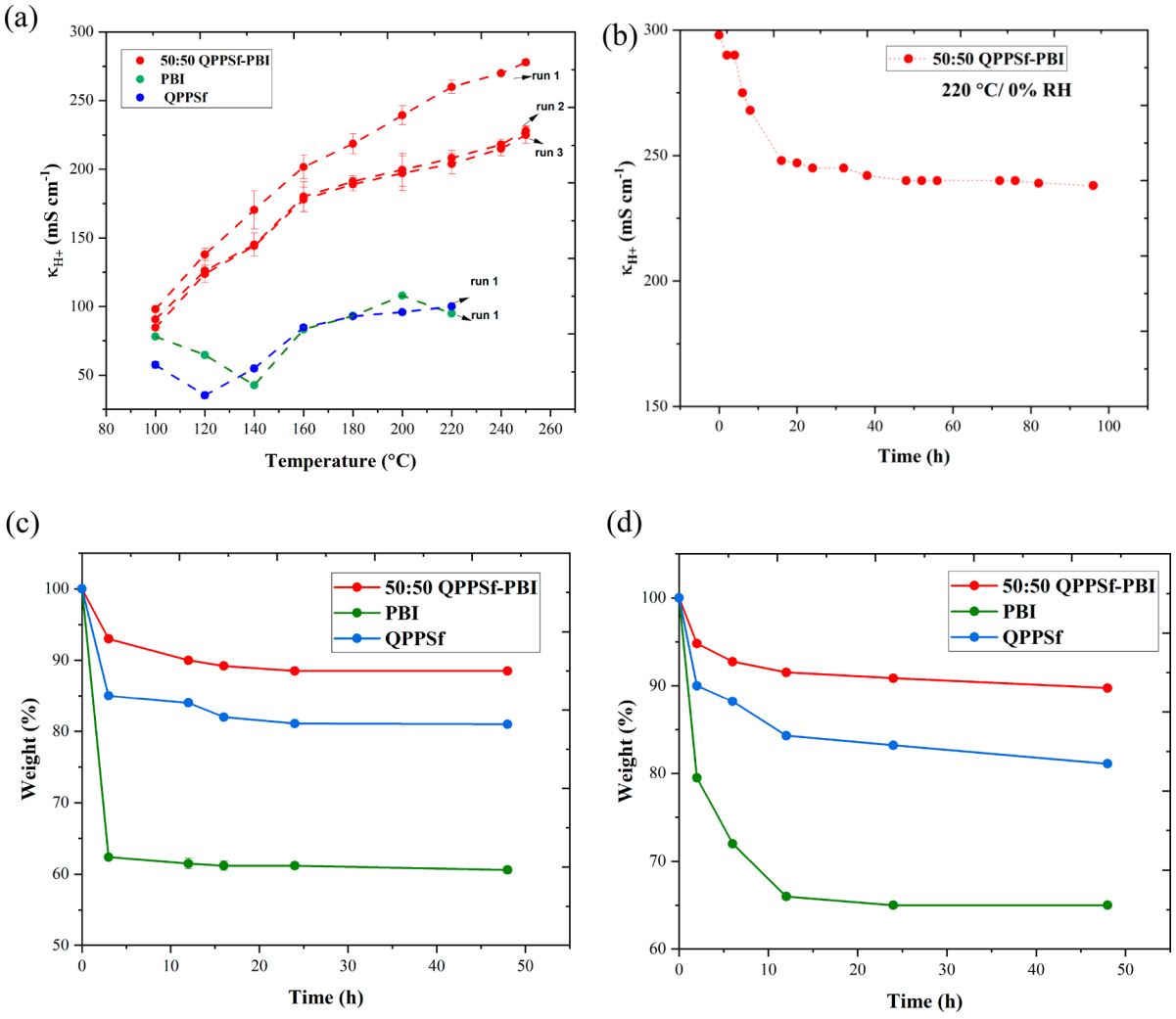

Figure 3. (a) In-plane κ_{H+} for PBI, QPPSf, and PBI−QPPSf (50:50) blend during temperature cycling from 100−250 °C and 0% RH. For each cycle temperature, the sample was brought back to 100 °C and increased back up to 250 °C. (b) In-plane κ_{H+} for QPPSf−PBI 50:50 for 96 h. (c) Percentage weight loss of membranes at 220 °C/0% RH. (d) Percentage weight loss of membranes at 80 °C/40% RH. (Note: the error bars are very small in the traces.)

their thermal stability and acid retention over time when operating the cell above 180 °C. Moving to higher cell temperatures can improve the redox kinetics in the IT-PEMFC,[26,32] while also creating a larger temperature gradient between the cell and external environment for heat rejection. Figure 3a shows the loss in κ_{H+} for PBI, QPPSf, and 50:50 QPPSf−PBI membranes during three thermal cycles in the temperature range of 100 to 250 °C. For the first cycle, the temperature was ramped to 250 °C. At the end of that cycle, the temperature was returned to 100 °C followed by ramping it back up to 250 °C. 50:50 QPPSf−PBI experienced about 20% drop in κ_{H+} after the first cycle and retention of κ_{H+} into the third cycle. PBI and QPPSf, on the other hand, ceased κ_{H+} after the first thermal cycle. To further assess the thermal stability of 50:50 QPPSf−PBI membrane, κ_{H+} was monitored at 220 °C and 0% RH, a challenging condition, over a 96 h period (see Figure 3b). Similar to Figure 3a, Figure 3b shows a 20% drop in κ_{H+} over 20 h followed by stable κ_{H+} of 0.24 S cm^{-1} over the next 76 h. At the challenging 220 °C temperature, it appears that there is some excess H_3PO_4 evaporation from the 50:50 QPPSf−PBI host. After that minor acid loss, this membrane blend stabilizes and provides a high κ_{H+} of 240 mS cm^{-1}.

To complement the κ_{H+} stability assessment of the membranes, Figure 3c reports the weight loss of the PBI, QPPSf, and 50:50 QPPSf−PBI at 220 °C up to 48 h. During that time, PBI lost 36% of its weight within the first two hours, whereas QPPSf and 50:50 QPPSf−PBI lost 15% and 7% of their initial weight, respectively. At the end of the 48 h test, PBI and QPPSf suffered 40% and 17% weight loss, while 50:50 QPPSf−PBI lost only 8% of its initial weight. The high acid loss of PBI was due to the excess free acid evaporating from the polymer. The total nH_3PO_4 B^{-1} retained after the 48 h stability test at 220 °C for all the membrane samples is given in Table 2. The 50:50 QPPSf−PBI membrane had the lowest acid loss per base. The high H_3PO_4 retention at the end of the stability test for 50:50 QPPSf−PBI indicates that this material can provide excellent κ_{H+} at the temperature of 220 °C for extended periods of time. Figure S13 reports the weight loss of the other QPPSf−PBI polymer blends at 220 °C/0% RH for 48 h, and this figure conveys that the other polymer blends only lose 17% to 20% of their initial weight during the thermal stability test. This result indicates that the other polymer blend membranes yield similar thermal stability to the QPPSf variant

DOI: 10.1021/acsaem.9b01802
ACS Appl. Energy Mater. 2020, 3, 573−585

Table 2. nH_3PO_4 B^{-1} values before and after Thermal and Humidity Stability Tests for PBI, QPPSf, and 50:50 QPPSf–PBI

Sample	nH_3PO_4 B^{-1}(initial)	nH_3PO_4 B^{-1} (after 48 hours at 220 °C/ 0% RH)	nH_3PO_4 B^{-1} (after 48 hours at 80 °C/ 40% RH)
PBI	9.4	5.6	5.1
QPPSf	9.3	7.7	7.9
50:50 QPPSf–PBI	7.9	6.3	7.3

and do not give the same level of stability as the 50:50 QPPSf–PBI variant.

Because the TGA data (Figure S14a) showed quaternary benzyl pyridinium groups in PSf starting to degrade at temperatures ≥200 °C, it was decided to assess if the quaternary benzyl pyridinium groups in the 50:50 QPPSf–PBI blend and QPPSf membranes without acid were stable at 220 °C through another experimental method. Both pristine QPPSf and 50:50 QPPSf–PBI membrane samples were exposed to 220 °C for 48 h. After this thermal treatment, the membranes were imbibed with H_3PO_4 and the in-plane κ_{H+} was measured at 25 °C, 50 °C, and 100 °C. The in-plane κ_{H+} values of these membranes after thermal treatment were compared against existing data sets of the membranes not exposed to 220 °C for 48 h. Figure S15 demonstrates that the 50:50 QPPSf–PBI blend had much better thermal stability over QPPSf by itself. 50:50 QPPSf–PBI lost just 10% of its initial weight, whereas QPPSf lost 22% of its initial weight after the thermal treatment, which is directly depicted in their in-plane κ_{H+} of these membrane samples, where QPPSf lost its entire initial κ_{H+}, whereas 50:50 QPPSf–PBI retained 98% of its initial κ_{H+}.

From Figures 3a–c, it is evident that the 50:50 QPPSf–PBI displayed reasonably good thermal stability at 220 °C in terms of acid retention and κ_{H+}. Furthermore, the TGA data (Figure S14) and weight loss data of pristine 50:50 QPPSf–PBI compared against pristine QPPSf (Figure S15) support that the 50:50 QPPSf–PBI membrane blend would be stable at the fuel cell operating temperature of 220 °C for a few days. But this temperature over a long period of time may cause slow degradation of quaternary benzyl pyridinium. However, the TGA indicates that temperatures at 200 °C or below would ensure stability of the quaternary benzyl pyridinium group.

The excellent acid retention and κ_{H+} at 220 °C for 48 h was attributed to the cationic group in the PC anchoring the phosphate type anions preventing H_3PO_4 evaporation which occurs in PBI membranes. Additionally, there appears to be a cooperative effect between PBI and QPPSf that prevents excess swelling of the membrane when incorporating H_3PO_4 that results in enhanced thermal stability and improved κ_{H+}. Recall that the QPPSf by itself swelled quite a bit when incorporating H_3PO_4. Taking this membrane variant above 200 °C resulted in further swelling and eventual dissolution. Another consideration for the excellent acid retention of 50:50 QPPSf–PBI is due to the condensation of H_3PO_4 to pyrophosphoric acid at 220 °C.[42] These high molecular weight acids are less volatile and cannot evaporate at 220 °C.

Finally, 50:50 QPPSf–PBI stability was assessed under the condition of 80 °C and 40% relative humidity (RH) by placing it in a BekkTech conductivity cell (4-point platinum probe with PTFE housing) situated in fuel cell hardware under humidity control (see Figure 3d). This condition was assessed because it is desirable for the 50:50 QPPSf–PBI to be flexible for fuel cell conditions at elevated temperatures and dry conditions (220 °C and 0% RH) and lower temperatures with moderate humidity (e.g., 80 °C and 40% RH).[26] At the lower temperature condition with humidity, it is known that water can supplant H_3PO_4 resulting in a κ_{H+} drop due to the loss of electrolyte.[20] Figure 3d shows that 50:50 QPPSf–PBI retained 93% of its weight over 48 h at 80 °C and 40% RH, while PBI only retained 65% of its weight (i.e., a 35% weight loss). QPPSf retained 82% of its weight. Similar to the thermal stability results, the good stability at 80 °C and 40% RH for 50:50 QPPSf–PBI signifies that there is a synergistic effect between PBI and the PC that assists H_3PO_4 retention in the presence of water vapor. Table 2 also gives the change in nH_3PO_4 B^{-1} for the different membrane variants after the humidity stability

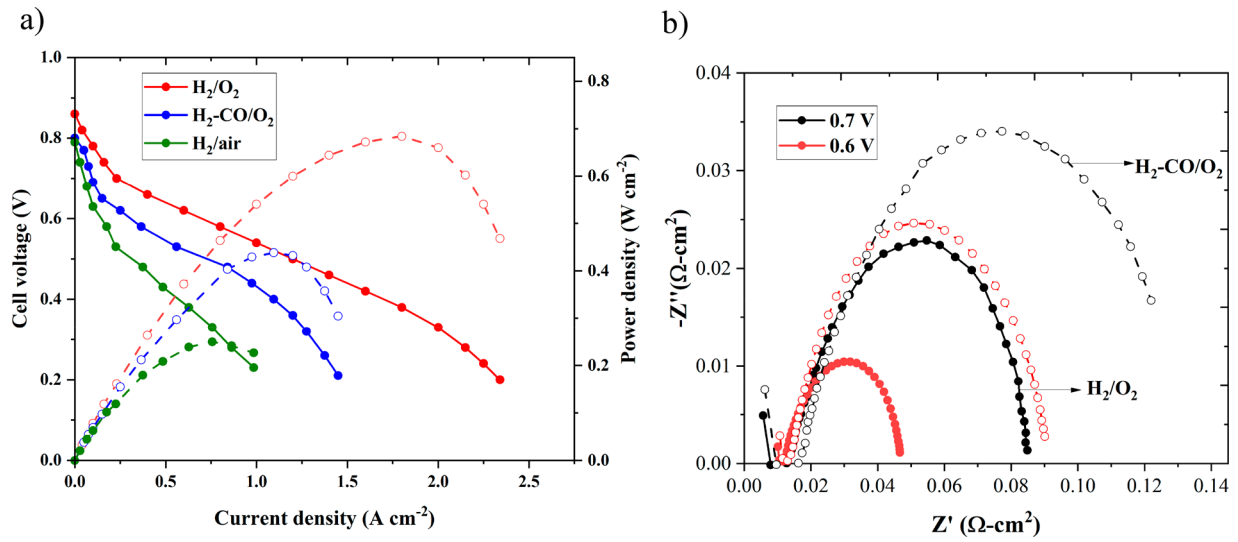

Figure 4. (a) Fuel cell polarization curve with H_2/O_2, and $H_2–CO/O_2$ with 50:50 QPPSf–PBI membrane with QPPSf GDEs (0.5 mg_{Pt} cm^{-2}) at 220 °C/0% RH with 161 kPa of back pressure on both the anode and cathode. (b) Nyquist plots of 50:50 QPPSf–PBI membrane with QPPSf electrodes at 220 °C/0% RH for H_2/O_2 (closed circle) and $H_2–CO/O_2$ (open circle).

DOI: 10.1021/acsaem.9b01802
ACS Appl. Energy Mater. 2020, 3, 573–585

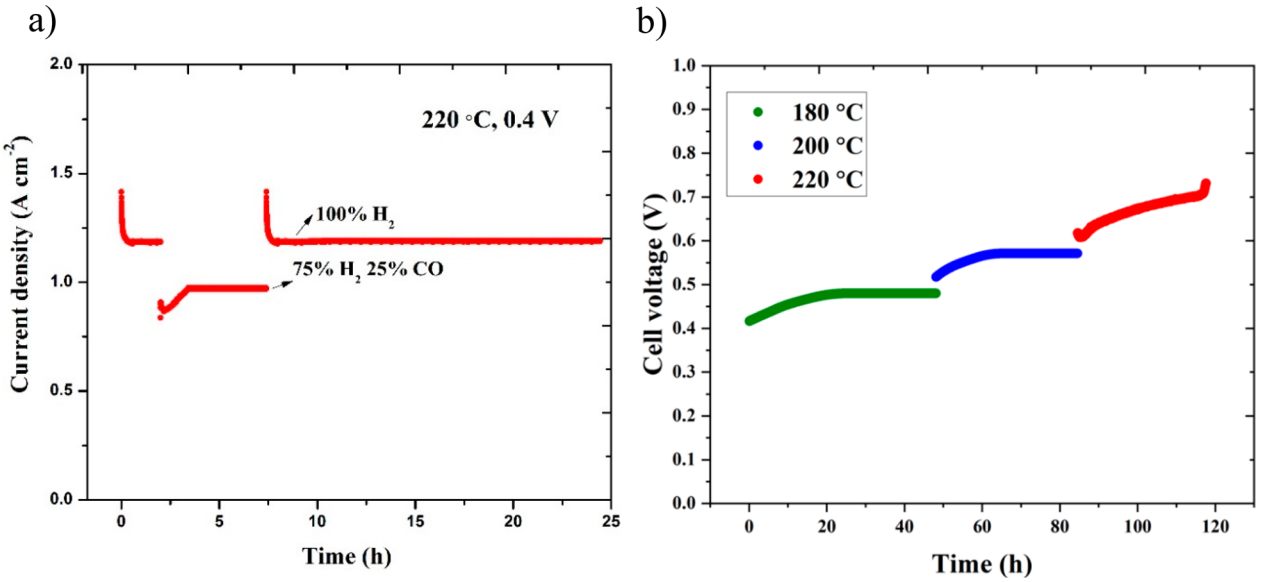

Figure 5. (a) 24-h stability test for 50:50 QPPSf–PBI membrane with QPPSf GDEs under H_2/O_2 and H_2–CO/O_2 at 220 °C/0% RH with 161 kPa of back pressure. (b) Cell voltage (vs) time at 0.2 A cm^{-2} for 50:50 QPPSf–PBI membrane with QPPSf ionomer binder at 180 °C, 200 °C, and 220 °C under H_2/O_2 and no back pressure.

test. Overall, 50:50 QPPSf–PBI shows excellent thermal stability (up to 220 °C) and resilience in the presence of water vapor (80 °C and 40% RH) making it a promising candidate for IT-PEMFCs that can operate robustly under a wide-range of temperatures and levels of humidification.

3.6. Fuel Cell Performance and CO Tolerance Stability. Figure 4a gives the IT-PEMFC polarization curve at 220 °C and 161 kPa of back pressure with 50:50 QPPSf–PBI membrane featuring GDEs that use a QPPSf ionomer binder and platinum (Pt) nanoparticle electrocatalyst decorated on higher surface area carbon (0.5 mg_{Pt} cm^{-2}). The polarization behavior was examined initially for dry H_2/O_2 and H_2/air (note: 3 independent MEAs were prepared with this configuration and evaluated with H_2/O_2 for repeatability—see Figure S16). The peak power density value for H_2/O_2 was 687 mW cm^{-2}, and for H_2/air it was 250 mW cm^{-2}. The H_2/O_2 values were competitive with the Los Alamos National Laboratory peer-reviewed reports that showed 870 mW cm^{-2} at 240 °C with a ceramic membrane and PC binder and 800 mW cm^{-2} at 180 °C with a PC membrane and binder (note: both of these demonstrations were with H_2/O_2).[24,26] Using electrochemical impedance spectroscopy (EIS; see Figure 4b), the high frequency resistance (HFR) was 0.01 to 0.015 Ω-cm^2 at 220 °C signaling that the 50:50 QPPSf–PBI membrane can withstand a high current density with a small ohmic overpotential. For example, 20 mV ohmic overpotential would occur if the cell was operated near 2 A cm^{-2}, which in this case was near the peak power density for this H_2/O_2 demonstration. However, the peak power density occurred near 0.3 to 0.35 V showing about 600 mV of polarization. Figure 4b demonstrates a 0.05 Ω-cm^2 to 0.075 Ω-cm^2 charge-transfer resistance when operating the cell at different current density values. These values are substantially higher than the HFR (due to ohmic resistances) in the cell and highlight that the IT-PEMFC needs some improvement with regard to electrode kinetics as the ohmic resistance has been minimized. A drawback to H_3PO_4 doped polymers for IT-PEMFCs is phosphate type anion adsorption to electrocatalyst surfaces that block sites for reactant adsorption and hindering reaction kinetics.[43,44]

Another important consideration for H_3PO_4-doped MEAs for IT-PEMFCs is that significant mass transfer resistances could occur if too much H_3PO_4 is present in the electrode layers. The liquid acid can flood the electrodes resulting in hindered reactant delivery to the electrode surfaces and compromised IT-PEMFC performance. Figure S17 shows a polarization curve using 50:50 QPPSf–PBI membrane and ionomer binder in the GDEs compared to 50:50 QPPSf–PBI membrane and a QPPSf ionomer binder only in the GDE. This material, 50:50 QPPSf–PBI, was shown to have greater H_3PO_4 uptake over QPPSf (see Table 1). Because there is more H_3PO_4 uptake with 50:50 QPPSf–PBI, there is significant mass transfer that hinders reactant delivery to the electrocatalyst surface, and thus, a peak power density of 100 mW cm^{-2} was only attained. At the same temperature, QPPSf ionomer binder shows better performance. Hence, removing PBI from electrode reduces the mass transfer resistance in the electrodes because there is less H_3PO_4 present that obfuscates delivery of reactant gas.

Figure S18a directly compares the fuel cell performance of an IT-PEMFC with different membrane separators: 50:50 QPPSf–PBI, PBI, and QPPSf membranes. This comparison was carried out at 180 °C and no back pressure to make sure the membranes were stable for attaining polarization curves. Figure S18a clearly shows that the 50:50 QPPSf–PBI membrane blend gave superior performance over the other membrane separators. It is important to note the MEAs for the 50:50 QPPSf–PBI and QPPSf demonstrations used QPPSf ionomer as the electrode binder. The PBI demonstration used PBI as the electrode ionomer binder. The 2.5× higher power density for the 50:50 QPPSf–PBI blend membrane separator was attributed to its higher ionic conductivity resulting in a lower ohmic drop. The higher ionic conductivity was substantiated by the lower HFR of 50:50 QPPSf–PBI membrane observed in Figure S18b from EIS experiments during the IT-PEMFC tests (note: the membrane thicknesses for each of these fuel cell runs ranged from 36 to 42 μm, and

DOI: 10.1021/acsaem.9b01802
ACS Appl. Energy Mater. 2020, 3, 573–585

hence, it is the conductivity of the membrane and not membrane thickness for influencing the HFR).

Figure S19 depicts the IT-PEMFC performance at different temperatures. These polarization curves are *iR* corrected and show that the redox kinetics are increasing when moving the cell to higher temperatures, which is another reason justifying higher temperature operation. Our future plans to improve the performance of IT-PEMFCs with the 50:50 QPPSf−PBI membrane will pursue tethered phosphonic acid groups to polymer backbones for the electrode ionomer binder used in electrode layers. Tethering the phosphonate groups to the polymer chain will reduce phosphate type anion adsorption to the electrocatalyst surface. Plus, there will be no need for doping H_3PO_4 into the electrode that causes liquid layers that block reactant delivery. The CMPSf used in this report can be converted into phosphonated polymers using established procedures in the literature.[45−47]

As previously mentioned, IT-PEMFCs can tolerate CO in the H_2 fuel stream and thus enable the use of low cost H_2 fuel. Hence, an IT-PEMFC demonstration was carried out with a blend of 75% H_2 and 25% CO as the fuel (see Figure 4a). The peak power density for H_2−CO/O_2 was 440 mW cm^{-2}. Figure 4b compares the Nyquist plots for H_2/O_2 and H_2−CO/O_2. It is clear from this figure that the charge-transfer kinetics increase by almost a factor of 2 resulting in the near 35% drop in fuel cell performance. CO present in the fuel stream dilutes the hydrogen reactant in addition to blocking the platinum catalyst surface. It is important to note that the HFR for the H_2−CO/O_2 was about the same (10 to 15 mΩ-cm^2) as H_2/O_2 indicating that the CO did not impact the membrane's resistance.

Finally, a 24-h stability evaluation was performed for the IT-PEMFC with a 0.4 V voltage hold and monitoring cell current density at 220 °C and 0% RH (see Figure 5a). During the stability assessment, the cell was originally operated on H_2/O_2 for 2 h, then switched to H_2−CO/O_2 for 6 h, and then switched back to H_2/O_2 for 16 h. Because of dynamic shifts in the cell, the IT-PEMFC current density always dropped quickly when switching the fuel, but then the cell was stable for several hours showing no decay in the current density at 0.4 V. More importantly, the cell almost completely recovered its original current density when switching back to H_2/O_2 indicating that the adsorbed CO on the electrocatalyst surface could be desorbed when pure H_2 was present in the anode. At the end of 24 h stability test, which featured exposure to CO, the polarization curve for H_2/O_2 was collected and it was within 95% of the original polarization curve collected with H_2/O_2) (see Figure S20). A drop in OCV was observed after the stability test. To understand the OCV drop, the hydrogen crossover at 220 °C was measured before and after the stability (see Figure S21). The difference in hydrogen crossover before and after the stability test was about 0.5 mA cm^{-2} indicating mixed overpotentials could not be the reason for the drop in the OCV. The drop in OCV after the 24 h stability assessment may be due to some residual carbon monoxide still being present in the IT-PEMFC.

Furthermore, a longer stability assessment was performed for the IT-PEMFC under a different protocol as reported by Li et al.[32] In this protocol, the cell was operated at a constant current at 0.2 A cm^{-2} and no back pressure was applied, and we evaluated the IT-PEMFC stability at different temperatures over 116 h. Before discussing these results, it is important to note that the IT-PEMFC with the 50:50 QPPSf−PBI membrane blend failed at 32 h at 0.2 A cm^{-2} at 220 °C and 161 kPa of back pressure. Because of this failure, which was related to the blended membrane breaking, it was decided to reassess stability at lower temperatures and no back pressures. Figure 5b shows that the 50:50 QPPSf−PBI membrane blend was stable for 48 h at 180 °C followed by 36 h of stability at 200 °C. Then, the cell temperature was raised to 220 °C and the cell failed after an additional 32 h—which was similar to the time it took for the cell to fail in the previous stability assessment. From our tensile test results, we observed that the 50:50 QPPSf−PBI membrane blend experienced a significant drop in mechanical strength when increasing the temperature to 220 °C (11.9 MPa at break to 1.8 MPa at break—see Figure S6b). Our future wok will look to overcome the membrane mechanical integrity failure mode for improving IT-PEMFC stability.

In summary, these experiments highlight the following salient points: (i) The 50:50 QPPSf−PBI can sustain a high current density with low polarization, and IT-PEMFC performance is currently limited by reaction kinetics. (ii) The IT-PEMFC can operate with reasonable power density when changing the anode feed composition to 75% H_2 and 25% CO (indicating reformate or syn gas can power the cell potentially). (iii) The QPPSf ionomer binder and 50:50 QPPSf−PBI PEM are stable within the cell at 220 °C up to 30 h with oxygen as the oxidant and over 80 h at 180 °C. (iv) The cell can recover its original performance when switching from H_2−CO fuel back to H_2 fuel showing that the CO adsorption effect is reversible.

4. CONCLUSION

A series of PC and PBI blends were successfully developed, and the 50:50 weight ratio of the blend showed exceptional in-plane κ_{H+} of 0.2 to 0.3 S cm^{-1} in the temperature range of 200 to 240 °C, while also displaying good mechanical properties (11.9 MPa at break) and thermal stability at 220 °C (less than 10% weight loss over 48 h). The excellent κ_{H+} of the 50:50 QPPSf−PBI was attributed to the PC promoting greater hydrogen bonding frustration and the PBI facilitating higher H_3PO_4 uptakes and a larger ε'. The 50:50 QPPSf−PBI membrane and QPPSf ionomer binder in GDEs gave a competitive power density of 680 mW cm^{-2} with H_2/O_2 at 220 °C, and it also enabled fuel cell performance with H_2−CO fuel (25% CO) − signaling that the IT-PEMFC with this class of materials is capable of running on H_2 from SRM. Additionally, this IT-PEMFC demonstration was carried out with an all-polymer MEA that is conducive to scalable manufacturing processes (e.g., roll-to-roll). It is important to note that the new materials displayed stability in the IT-PEMFC for about 30 h at the challenging temperature of 220 °C and that the fuel cell performance could be recovered when switching back to H_2 fuel from H_2−CO fuel. However, 50:50 membrane blend was shown to mechanically fail in the fuel cell at 220 °C when hitting 30 h of operation. Additional stability tests revealed that cell stability could be achieved over 80 h by operating the fuel cell at a lower temperature of 180 °C. Impedance analysis revealed that the low-resistant membranes can withstand a high current. Future efforts will focus on ionomer binder development for IT-PEMFCs to overcome mass transfer resistances and to make the membrane blends mechanically stable at higher temperatures (e.g., 220 °C) for longer periods of time.

DOI: 10.1021/acsaem.9b01802
ACS Appl. Energy Mater. 2020, 3, 573−585

■ ASSOCIATED CONTENT

Supporting Information

The Supporting Information is available free of charge at https://pubs.acs.org/doi/10.1021/acsaem.9b01802.

In-plane κ_{H+} of H_3PO_4-doped QPPSf−PBI blends at different ratios, NMR analysis of CMPSf and QPPSf, physical and mechanical properties of H_3PO_4-doped QPPSf−PBI blends, physical properties of 50:50 CMPSf−PBI blend, in-plane and through-plane κ_{H+} comparison for 50:50 QPPSf−PBI membrane, structural characterization of 50:50 QPPSf−PBI using SEM, average of n = 3 MEAs (independently prepared) fuel cell polarization curves with 50:50 QPPSf−PBI membrane with QPPSf ionomer binder in the electrode layers, fuel cell performance of 50:50 QPPSf−PBI membrane with 50:50 QPPSf−PBI and QPPSf as the ionomer binders, fuel cell performance comparison of PBI, QPPSf, and 50:50 QPPSf−PBI membranes at 180 °C/0% RH, *iR*-corrected polarization curves for QPPSf−PBI 50:50 membrane with QPPSf ionomer binder at different temperatures, hydrogen crossover determination before and after stability tests (PDF)

■ AUTHOR INFORMATION

Corresponding Author

*Christopher G. Arges e-mail: carges@lsu.edu.

ORCID

Gokul Venugopalan: 0000-0002-7332-4300

Geoffrey M. Geise: 0000-0002-5439-272X

Christopher G. Arges: 0000-0003-1703-8323

Notes

The authors declare no competing financial interest.

■ ACKNOWLEDGMENTS

PI Arges acknowledges financial support for this work from LSU Lift^2, Louisiana Board of Regents (Proof-of-Concept/Prototype Initiative), 3M Non-Tenured Faculty Award, and start-up funds provided by the Cain Department of Chemical Engineering at LSU. He also wishes to thank Dorin Boldor and Kerry Dooley for the use of their INSITRON and TGA instruments, respectively and Shri Sankar Subramanian and Vijay Ramani at Washington University St. Louis for assisting in the high temperature tensile test (ONR DURIP supported the acquisition of equipment for the high temperature tensile test). The LSU Shared Instrumentation Facilities and NMR spectrometers in the Department of Chemistry contributed to this work. We thank Dongmei Cao for assisting in the EDX mapping experiment using the SEM. Sarah Livingston's contribution to this project was supported by a NSF REU (Award # 1560305). Geoffrey Geise acknowledges partial support for this work from the National Science Foundation under Grant No. CBET-1752048. Kevin Chang acknowledges support from the Volkswagen Group of North America Fellowship.

■ REFERENCES

(1) Zhang, L.; Chae, S.-R.; Hendren, Z.; Park, J.-S.; Wiesner, M. R. Recent Advances in Proton Exchange Membranes for Fuel Cell Applications. *Chem. Eng. J.* **2012**, *204*−*206*, 87−97.

(2) Hickner, M. A.; Ghassemi, H.; Kim, Y. S.; Einsla, B. R.; McGrath, J. E. Alternative Polymer Systems for Proton Exchange Membranes (PEMs). *Chem. Rev.* **2004**, *104* (10), 4587−4612.

(3) Papageorgopoulos, D. Fuel Cell R&D Overview; **2019**, 1−33. https://www.hydrogen.energy.gov/pdfs/review19/plenary_fuel_cell_papageorgopoulos_2019.pdf.

(4) U.S. Department of Energy, Hydrogen Production Tech Team Roadmap; **2017**, 1−55. https://www.energy.gov/sites/prod/files/2017/11/f46/HPTT%20Roadmap%20FY17%20Final_Nov%202017.pdf.

(5) Rosli, R. E.; Sulong, A. B.; Daud, W. R. W.; Zulkifley, M. A.; Husaini, T.; Rosli, M. I.; Majlan, E. H.; Haque, M. A. A Review of High-Temperature Proton Exchange Membrane Fuel Cell (HT-PEMFC) System. *Int. J. Hydrogen Energy* **2017**, *42* (14), 9293−9314.

(6) Cheng, Y.; Zhang, J.; Lu, S.; Kuang, H.; Bradley, J.; De Marco, R.; Aili, D.; Li, Q.; Cui, C. Q.; Jiang, S. P. High CO Tolerance of New SiO2 Doped Phosphoric Acid/Polybenzimidazole Polymer Electrolyte Membrane Fuel Cells at High Temperatures of 200−250 °C. *Int. J. Hydrogen Energy* **2018**, *43* (49), 22487−22499.

(7) Glipa, X.; Bonnet, B.; Mula, B.; Jones, D. J.; Rozière, J. Investigation of the Conduction Properties of Phosphoric and Sulfuric Acid Doped Polybenzimidazole. *J. Mater. Chem.* **1999**, *9* (12), 3045−3049.

(8) Pilinski, N.; Rastedt, M.; Wagner, P. Investigation of Phosphoric Acid Distribution in PBI Based HT-PEM Fuel Cells. *ECS Trans.* **2015**, *69*, 323−335.

(9) Xiao, L.; Zhang, H.; Scanlon, E.; Ramanathan, L. S.; Choe, E.-W.; Rogers, D.; Apple, T.; Benicewicz, B. C. High-Temperature Polybenzimidazole Fuel Cell Membranes via a Sol-Gel Process. *Chem. Mater.* **2005**, *17* (21), 5328−5333.

(10) Kawahara, M.; Morita, J.; Rikukawa, M.; Sanui, K.; Ogata, N. Synthesis and Proton Conductivity of Thermally Stable Polymer Electrolyte: Poly(Benzimidazole) Complexes with Strong Acid Molecules. *Electrochim. Acta* **2000**, *45* (8), 1395−1398.

(11) Asensio, J. A.; Sánchez, E. M.; Gómez-Romero, P. Proton-Conducting Membranes Based on Benzimidazole Polymers for High-Temperature PEM Fuel Cells. A Chemical Quest. *Chem. Soc. Rev.* **2010**, *39* (8), 3210−3239.

(12) Mack, F.; Aniol, K.; Ellwein, C.; Kerres, J.; Zeis, R. Novel Phosphoric Acid-Doped PBI-Blends as Membranes for High-Temperature PEM Fuel Cells. *J. Mater. Chem. A* **2015**, *3* (20), 10864−10874.

(13) Han, M.; Zhang, G.; Liu, Z.; Wang, S.; Li, M.; Zhu, J.; Li, H.; Zhang, Y.; Lew, C. M.; Na, H. Cross-Linked Polybenzimidazole with Enhanced Stability for High Temperature Proton Exchange Membrane Fuel Cells. *J. Mater. Chem.* **2011**, *21* (7), 2187−2193.

(14) Li, Q.; Pan, C.; Jensen, J. O.; Noyé, P.; Bjerrum, N. J. Cross-Linked Polybenzimidazole Membranes for Fuel Cells. *Chem. Mater.* **2007**, *19* (3), 350−352.

(15) Hoel, D.; Grunwald, E. High Protonic Conduction of Polybenzimidazole Films. *J. Phys. Chem.* **1977**, *81* (22), 2135−2136.

(16) Gasteiger, H. A.; Kocha, S. S.; Sompalli, B.; Wagner, F. T. Activity Benchmarks and Requirements for Pt, Pt-Alloy, and Non-Pt Oxygen Reduction Catalysts for PEMFCs. *Appl. Catal., B* **2005**, *56* (1), 9−35.

(17) Yandrasits, M.; Lindell, M.; Schaberg, M.; Kurkowski, M. Increasing Fuel Cell Efficiency by Using Ultra-Low Equivalent Weight Ionomers. *Electrochem. Soc. Interface* **2017**, *26* (1), 49−53.

(18) Houchins, C.; Kleen, G. J.; Spendelow, J. S.; Kopasz, J. P.; Peterson, D. E. H.; Garland, N. L.; Ho, D. L.; Marcinkoski, J.; Martin, K.; Tyler, R. U.S. DOE Progress Towards Developing Low-Cost, High Performance, Durable Polymer Electrolyte Membranes for Fuel Cell Applications. In *Membranes* **2012**, *2*, 855.

(19) Wang, J.; Zhao, Y.; Setzler, B. P.; Rojas-Carbonell, S.; Yehuda, C. B.; Amel, A.; Page, M.; Wang, L.; Hu, K.; Shi, L. Poly (Aryl Piperidinium) Membranes and Ionomers for Hydroxide Exchange Membrane Fuel Cells. *Nature Energy* **2019**, *4* (5), 392.

(20) Lee, A. S.; Choe, Y.-K.; Matanovic, I.; Kim, Y. S. The Energetics of Phosphoric Acid Interactions Reveals a New Acid Loss Mechanism. *J. Mater. Chem. A* **2019**, *7* (16), 9867−9876.

(21) Zhang, J.; Zhang, J.; Bai, H.; Tan, Q.; Wang, H.; He, B.; Xiang, Y.; Lu, S. A New High Temperature Polymer Electrolyte Membrane

DOI: 10.1021/acsaem.9b01802
ACS Appl. Energy Mater. 2020, 3, 573−585

Based on Tri-Functional Group Grafted Polysulfone for Fuel Cell Application. *J. Membr. Sci.* **2019**, *572*, 496−503.
(22) Yang, J.; Li, Q.; Jensen, J. O.; Pan, C.; Cleemann, L. N.; Bjerrum, N. J.; He, R. Phosphoric Acid Doped Imidazolium Polysulfone Membranes for High Temperature Proton Exchange Membrane Fuel Cells. *J. Power Sources* **2012**, *205*, 114−121.
(23) Bai, H.; Peng, H.; Xiang, Y.; Zhang, J.; Wang, H.; Lu, S.; Zhuang, L. Poly(Arylene Piperidine)s with Phosphoric Acid Doping as High Temperature Polymer Electrolyte Membrane for Durable, High-Performance Fuel Cells. *J. Power Sources* **2019**, *443*, 227219.
(24) Lee, K.-S.; Maurya, S.; Seung Kim, Y.; Kreller, C. R.; Wilson, M. S.; Larsen, D.; Elango Elangovan, S.; Mukundan, R. Intermediate Temperature Fuel Cells via an Ion-Pair Coordinated Polymer Electrolyte. *Energy Environ. Sci.* **2018**, *11* (4), 979−987.
(25) Arges, C. G.; Zhang, L. Anion Exchange Membranes' Evolution toward High Hydroxide Ion Conductivity and Alkaline Resiliency. *ACS Appl. Energy Mater.* **2018**, *1* (7), 2991−3012.
(26) Lee, K.-S.; Spendelow, J. S.; Choe, Y.-K.; Fujimoto, C.; Kim, Y. S. An Operationally Flexible Fuel Cell Based on Quaternary Ammonium-Biphosphate Ion Pairs. *Nature energy* **2016**, *1* (9), 16120.
(27) Arges, C. G.; Parrondo, J.; Johnson, G.; Nadhan, A.; Ramani, V. Assessing the Influence of Different Cation Chemistries on Ionic Conductivity and Alkaline Stability of Anion Exchange Membranes. *J. Mater. Chem.* **2012**, *22* (9), 3733−3744.
(28) Bartley, P. G.; Begley, S. B. A New Technique for the Determination of the Complex Permittivity and Permeability of Materials. *In 2010 IEEE Instrumentation Measurement Technology Conference Proceedings* **2010**, 54−57.
(29) Luo, H.; Chang, K.; Bahati, K.; Geise, G. M. Engineering Selective Desalination Membranes via Molecular Control of Polymer Functional Groups. *Environ. Sci. Technol. Lett.* **2019**, *6*, 462.
(30) Chang, K.; Geise, G. M. Dielectric Permittivity Properties of Hydrated Polymers: Measurement and Connection to Ion Transport Properties. *Ind. Eng. Chem. Res.* **2019**, DOI: 10.1021/acs.iecr.9b03950.
(31) Chen, L.-F.; Ong, C. K.; Neo, C. P.; Varadan, V. V.; Varadan, V. K. *Microwave Electronics: Measurement and Materials Characterization*; John Wiley & Sons, 2004.
(32) Aili, D.; Zhang, J.; Jakobsen, M. T. D.; Zhu, H.; Yang, T.; Liu, J.; Forsyth, M.; Pan, C.; Jensen, J. O.; Cleemann, L. N.; Jiang, S. P.; Li, Q. Exceptional Durability Enhancement of PA/PBI Based Polymer Electrolyte Membrane Fuel Cells for High Temperature Operation at 200 °C. *J. Mater. Chem. A* **2016**, *4* (11), 4019−4024.
(33) Sata, T. *Ion Exchange Membranes: Preparation, Characterization, Modification and Application*; Royal Society of chemistry, 2007.
(34) Prabhakaran, V.; Arges, C. G.; Ramani, V. In Situ Fluorescence Spectroscopy Correlates Ionomer Degradation to Reactive Oxygen Species Generation in an Operating Fuel Cell. *Phys. Chem. Chem. Phys.* **2013**, *15* (43), 18965−18972.
(35) Yang, J.; Aili, D.; Li, Q.; Cleemann, L. N.; Jensen, J. O.; Bjerrum, N. J.; He, R. Covalently Cross-Linked Sulfone Polybenzimidazole Membranes with Poly(Vinylbenzyl Chloride) for Fuel Cell Applications. *ChemSusChem* **2013**, *6* (2), 275−282.
(36) Kim, Y. S.; Pivovar, B. S. The Membrane−Electrode Interface in PEFCs III. The Effect of Methanol Concentration in DMFCs. *J. Electrochem. Soc.* **2010**, *157* (11), B1608−B1615.
(37) Vilčiauskas, L.; Tuckerman, M. E.; Bester, G.; Paddison, S. J.; Kreuer, K.-D. The Mechanism of Proton Conduction in Phosphoric Acid. *Nat. Chem.* **2012**, *4* (6), 461−466.
(38) Melchior, J.-P.; Majer, G.; Kreuer, K.-D. Why Do Proton Conducting Polybenzimidazole Phosphoric Acid Membranes Perform Well in High-Temperature PEM Fuel Cells? *Phys. Chem. Chem. Phys.* **2017**, *19* (1), 601−612.
(39) Chang, K.; Luo, H.; Geise, G. M. Water Content, Relative Permittivity, and Ion Sorption Properties of Polymers for Membrane Desalination. *J. Membr. Sci.* **2019**, *574*, 24−32.
(40) Schechter, A.; Savinell, R. F.; Wainright, J. S.; Ray, D. #2#1 and #2#1 NMR Study of Phosphoric Acid−Doped Polybenzimidazole under Controlled Water Activity. *J. Electrochem. Soc.* **2009**, *156* (2), B283−B290.
(41) Dippel, T.; Kreuer, K. D.; Lassegues, J. C.; Rodriguez, D. Proton Conductivity in Fused Phosphoric Acid; A 1H/31P PFG-NMR and QNS Study. *Solid State Ionics* **1993**, *61* (1−3), 41−46.
(42) Krueger, R. A.; Vilčiauskas, L.; Melchior, J.-P.; Bester, G.; Kreuer, K.-D. Mechanism of Efficient Proton Conduction in Diphosphoric Acid Elucidated via First-Principles Simulation and NMR. *J. Phys. Chem. B* **2015**, *119* (52), 15866−15875.
(43) Myles, T.; Bonville, L.; Maric, R. Catalyst, Membrane, Free Electrolyte Challenges, and Pathways to Resolutions in High Temperature Polymer Electrolyte Membrane Fuel Cells. *Catalysts* **2017**, *7* (1), 16.
(44) Mack, F.; Galbiati, S.; Gogel, V.; Jörissen, L.; Zeis, R. Evaluation of Electrolyte Additives for High-Temperature Polymer Electrolyte Fuel Cells. *ChemElectroChem* **2016**, *3* (5), 770−773.
(45) Jakoby, K.; Peinemann, K. V.; Nunes, S. P. Palladium-Catalyzed Phosphonation of Polyphenylsulfone. *Macromol. Chem. Phys.* **2003**, *204* (1), 61−67.
(46) Abu-Thabit, N. Y.; Ali, S. A.; Zaidi, S. J. New Highly Phosphonated Polysulfone Membranes for PEM Fuel Cells. *J. Membr. Sci.* **2010**, *360* (1−2), 26−33.
(47) Cabasso, I.; Jagur-Grodzinski, J.; Vofsi, D. Synthesis and Characterization of Polymers with Pendent Phosphonate Groups. *J. Appl. Polym. Sci.* **1974**, *18* (7), 1969−1986.

DOI: 10.1021/acsaem.9b01802
ACS Appl. Energy Mater. 2020, 3, 573−585